(Received 11 January 2024, Accepted 19 May 2024, Scheduled 29 May 2024)

Analysis of Slot Antenna Performance for On-Body to In-Body Channel Characterization

T. N. Suresh Babu[1], Thirumaraiselvan Packirisamy[1,*], Priya Anumuthu[2], and Muthukannan Pethaperumal[3]

[1] *Adhiparasakthi Engineering College, Melmaruvathur, India*
[2] *B. S. Abdur Rahman Crescent Institute of Science and Technology, Chennai, India*
[3] *D. Y. Patil Deemed to be University, Navi Mumbai, India*

ABSTRACT: The propagation study of electromagnetic (EM) waves within a human body is becoming essential due to the growing demand for the design and development of implantable sensing nodes in a body area network (BAN). Many researchers are interested in contributing to the development of propagation models in the ultra-wideband (UWB), i.e., 3.1 to 10.6 GHz, for biomedical applications, as well as the license-free Industrial, Scientific, and Medical (ISM) band. This kind of propagation model is essential in order to design and develop UWB transceivers for in-body, on-body, and off-body communications. This paper looks at the possibility of using a stepped slot patch antenna with a copper ground plane as either an off-body or on-body antenna by comparing measurements taken on a liquid human phantom. In addition, we use the empirical data to propose a statistical model.

1. INTRODUCTION

The development of wireless sensing nodes for body area network (BAN) could enable sophisticated medical facilities for people residing in remote places. In addition, this will make the continuous monitoring of elderly people easier and more efficient from anywhere, even from our workplaces. As a result, performing research on the design and development of monitoring devices, such as wireless sensors for human bio-signals, is gaining popularity these days [1]. Ultra-wideband (UWB) has been released for biomedical applications to meet the high data rate channel requirements of applications like in-body images or videos [2]. However, the UWB channel through human tissues is not completely characterized for medical applications, especially for on-body or off-body-to-in-body communication. In UWB, this necessitates a deeper knowledge of EM wave propagation in human tissues.

Measuring the characteristics of UWB channels within living human organisms is difficult from a practical standpoint. Hence, the collection of empirical data from in vivo measurements with animals or human tissue mimicking phantoms is an alternative solution. On the other hand, channel models may also be developed to foresee the transmission of radio waves inside the human body based on the above experimental data or numerically. Many of the published BAN channel measurements and models only describe ISM and narrow band channels.

Researchers have proposed only a few propagation models to characterize the UWB channels for on-body or off-body-to-in-body communication. The very first UWB channel model [3] examined the viability of using the 3.4–4.8 GHz frequency band as a channel between in-body and on-body transceivers. The authors conducted numerical simulations based on the frequency-dependent finite difference time domain (FDTD) method. The authors in [4] obtained simulated data with a voxel model of an adult male, deriving this model from the results. The above voxel model is available at the National Institute of Information and Communications Technology, Japan. The researchers developed the voxel model using magnetic resonance imaging (MRI) data and included almost fifty types of human tissues. For this model, simulated data were obtained at each of the randomly selected twenty locations in the chest at depths ranging from 0.6 cm to 1.8 cm.

The above numerical models need the complex structure of human models and consume more time. In addition, researchers have proposed a few empirical models within the frequency range of 1 GHz to 6 GHz at a depth of 0.5 cm–12 cm in the chest, as described in [5] and [6]. Simulations using time-domain finite integration techniques (FIT) obtained the existing data that support these statistical models. In the above case, a voxel model of the human body was used to describe the human body model, incorporating frequency-dependent dielectric properties [7].

A function of frequency determines the attenuation that EM waves experience as they travel through space. In [8], researchers improved the previous model by incorporating the frequency-dependent nature of UWB signals. In [9], researchers proposed another empirical model for in-body to on-body channels in the lower UWB, i.e., 1–6 GHz. This model is applicable to the human abdomen region only. The simulation was conducted first for several implanted node positions in the abdomen region of an anatomical model at

* Corresponding author: Packirisamy Thirumaraiselvan (thirumarai@hotmail.com).

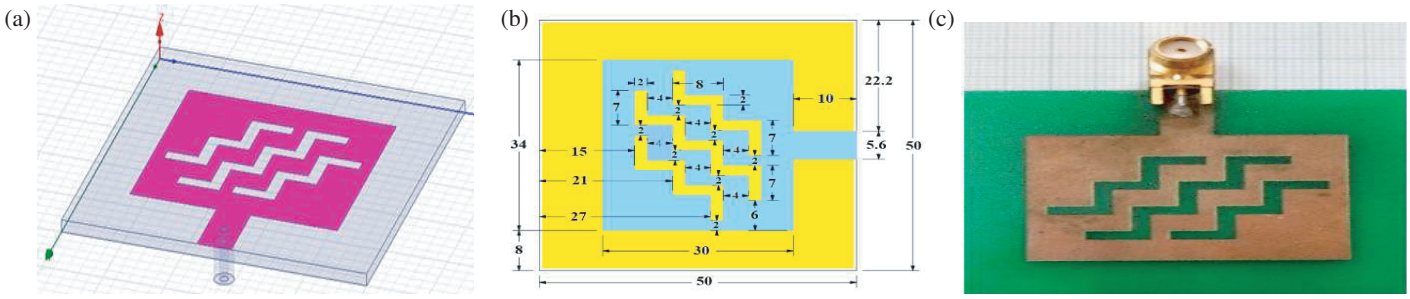

FIGURE 1. The proposed stepped slot multi-band patch antenna. (a) Simulated 3-D stepped slot patch antenna. (b) Dimensions of stepped slot patch. (c) Fabricated prototype antenna.

a depth of 0.1 cm–1.5 cm. The authors derived the above statistical model after analyzing the simulated data. After a computational analysis, they also improved the model to determine the path loss for a digestive tract in the frequency range of 3.4–4.8 GHz. The model is highly applicable to the in-body biomedical application known as capsule endoscopy [10]. To avoid conducting unethical in vivo measurements using the human body, experiments were conducted with anesthetized porcine subjects. The researchers placed the transmitting antenna at various locations inside the body, while keeping the receiving antenna on the surface of the body. They developed a path loss model from the measurements taken. The first in-body to on-body UWB channel path loss model from in-vivo measurements was conducted with animal subjects [11]. This path loss model provides good results within the frequency range of 1–6 GHz and for the implanted node locations within the depths of 50 mm–160 mm.

Signals lose a lot of power when they travel through tissue layers and bones in a body area network with implanted sensors because they travel in multiple directions [12]. In addition, modern hospital building structures include concrete floors and metal frames that support drop ceilings made of acoustical materials. Within the rooms, patients' state can be checked using beds, iron tables, trolleys, and medical equipment. These objects attenuate radio waves. The authors in [14] describe a geometrical optics-based model to anticipate propagation inside buildings with the aim of creating personal communication systems.

Numerical models are necessary to analyze path loss for a specific set of transmitter and receiver locations. These models are based on the dielectric and physical properties of structures outside the body and tissues nearby where the transceivers are located. According to [15, 16], raytracing is the preferred method for conducting numerical simulations because it takes into account site-specific information, which is crucial for predicting signal attenuation. The authors predict the path loss of an on-body to in-body UWB channel using a UWB antenna design and numerical channel model [17].

Researchers reported a UWB antenna with stable and omnidirectional radiation properties and fine tuning of the feed in [18]. The set of slots comprising pi, triangular, and circular shapes in the patch increases the gain by approximately up to 2 dBi. Without thick and complex designs, they help stabilize the radiation patterns by reducing side lobe levels and nulls in the broadside [19]. It was possible to make a dual- or triple-band patch antenna by adding U-slots to the patch of a broadband antenna [20]. The authors utilized this method for the L-probe-fed patch, M-probe-fed patch, coaxial-fed stacked patches, and aperture-coupled stacked patches. Researchers have created a brand-new monopole antenna with dual-band notched features for UWB use. It has a square radiating patch with a modified T-shaped slot, a ground plane with two E-shaped slots, and a W-shaped conductor-backed plane [21]. Printed elliptical/circular slot antennas for UWB applications, featuring feeds on the same and different sides, are presented in [22]. The fractal implementation of an antenna improves the impedance bandwidth at least twice compared to conventional printed slot antennas [23].

For enhanced performance on bio-tissue, an antenna design connects WBAN with wireless technologies, covers three bands, and features a perfect conducting metal plate, designed for on-body to off-body communication [24]. A compact UWB antenna with twisted F slots offers an ultra-wideband 3.1 to 10.6 GHz with a modified ground plane, evaluated using a three-layered rectangular phantom model [25]. In [26], authors suggest using one-layer and three-layered phantoms to simulate implant antennas in the ISM band.

This paper characterises an on-body to in-body channel in UWB using a stepped slot patch antenna and studies its path loss characteristics using a honey-based liquid phantom. In addition, simulations were performed using BANsim [16], to predict the path loss in the above scenario for comparison.

2. ANTENNA DESIGN AND PARAMETRIC ANALYSIS

Using a high-frequency structure simulator (HFSS), we design the proposed multi-band suspended stepped slot microstrip patch antenna with dimensions of 50 mm × 50 mm × 1.6 mm, along with the feeding structure. Figure 1 demonstrates the basic geometry and fabricated prototype of the antenna. The antenna is developed on a FR4 epoxy substrate with a relative dielectric constant (ε_r) of 4.4, a loss tangent of 0.02, and a height of 1.6 mm, with a copper ground plane on the substrate's lower side.

The fabricated prototype was characterized in the frequency range of 30 kHz to 9 GHz using a microwave vector network analyzer (FieldFox N9925A). Figure 2 illustrates the return loss

TABLE 1. Operating frequency band of proposed antenna in free space and phantom.

Band of operation (GHz)	Return Loss (dB) (Free space)	Return Loss (dB) (Human body phantom)
5.46–5.68	−24.25	−20.45
7.08–7.3	−20.47	−17.4
8.34–9.15	−34.06	−26.5

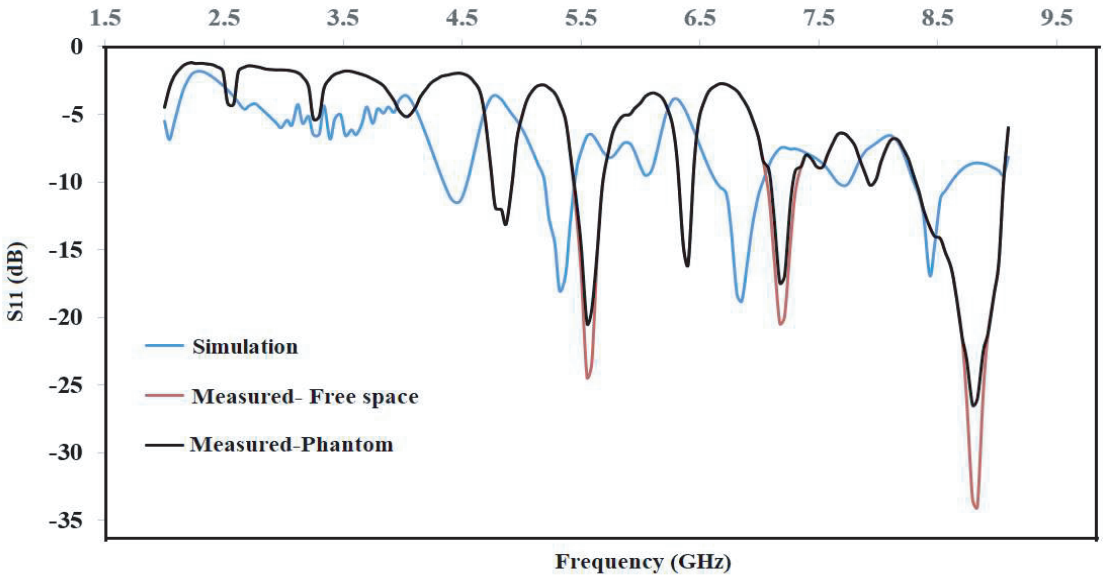

FIGURE 2. Return loss of the proposed antenna in free space and within body Phantom.

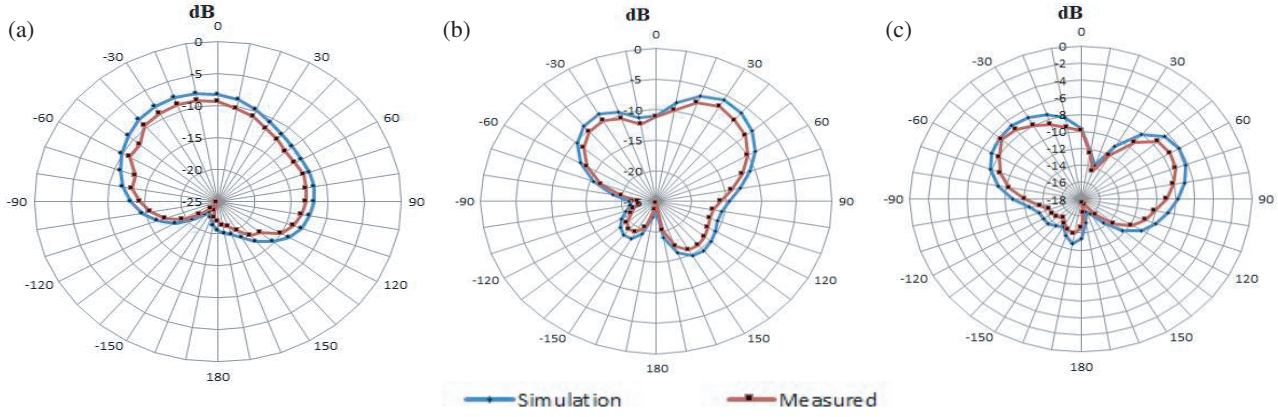

FIGURE 3. Gain radiation pattern of the proposed antenna for (a) 5.6 GHz, (b) 7.2 GHz, (c) 8.5 GHz.

S_{11} versus frequency curve for the proposed antenna, which was simulated and measured in both free space and human phantom. It is evident in Figure 2 that there are multiple resonances, each providing a broad bandwidth according to the simulation and practical results. Furthermore, the coupling of human body phantoms with the resonant frequency leads to a noticeable difference in the variation of return loss compared to free space. Table 1 shows the comparison of return losses at various resonant frequency bands measured in free space and within the human body phantom.

To meet the far-field requirement and eliminate outside interference, we test the planned antenna prototype by measuring its radiation patterns in an anechoic chamber at a distance of 1.5 m. Figure 3 shows the respective radiation patterns of the proposed antenna at 5.6, 7.2, and 8.5 GHz. The proposed antenna exhibits a butterfly-shaped radiation pattern at 8.5 GHz, while demonstrating good unidirectional radiation characteristics at the operating frequencies of 5.6 and 7.2 GHz. Table 2 shows the performance comparison between the simulated and measured peak gains of the proposed antenna. The simulated

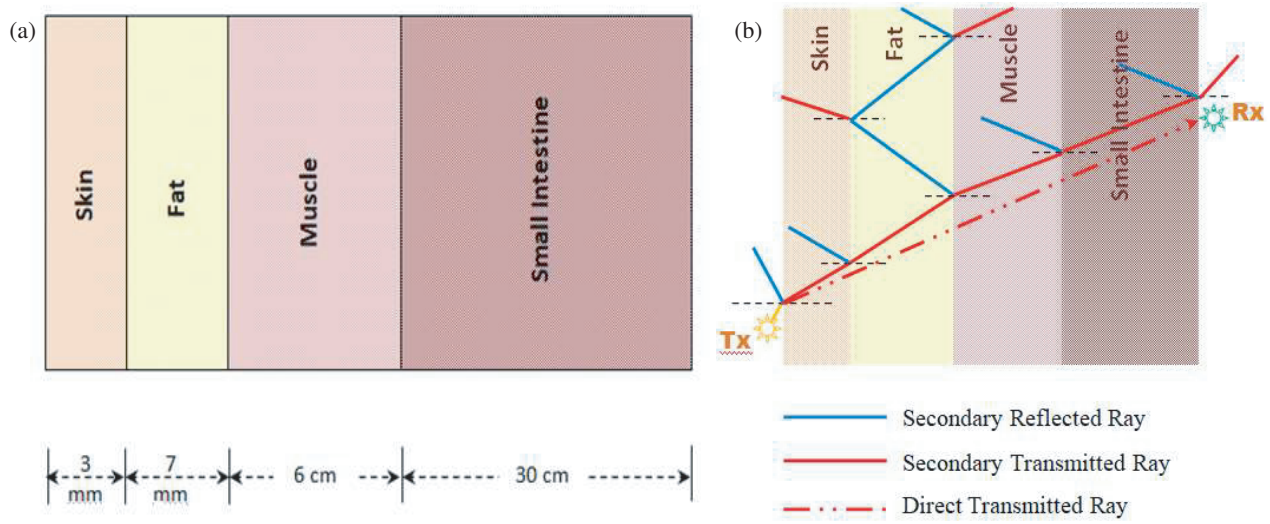

FIGURE 4. Cross section and Ray tracing in tissue layers of human abdomen model.

TABLE 2. Realized peak gain of the proposed antenna.

Operating frequency (GHz)	Realized peak gain (dBi)	
	Simulation	Measurement
56	−8.22	−9.42
7.2	−5.84	−7.01
8.5 directed at 60°	−6.03	−7.23
8.5 directed at 40°	−6.64	−7.84

and measured outcomes show a good agreement. The small difference between the two sets of results is due to many factors, including antenna fabrication tolerances, vector network analyzer calibration, and possibly multiple reflections in the measurement environment.

3. SCENARIO FOR SIMULATION

Numerical simulations have been performed using BANsim [16], a raytracing based simulator. A layer of heterogeneous tissue, regarded as a single, multi-layered object, serves as the propagation channel between the transmitter and receiver. Figure 4(a) shows the use of a four-layer model of a human abdomen for numerical simulations. The simulation parameters include the depth of penetration and respective tissue layers depending on the location of the receiving antenna.

There is no direct channel for on-body vs. in-body communications since the in-body antenna will be an implantable one. Hence, a Direct Transmitted Ray (DTR) path is used instead of the Line of Sight (LOS) path, and the intensity of the electric field of the DTR from the transmitter to the receiver is assessed with the inclusion of the ABCD matrix [13] in the computation of the scattering coefficient. After the transmitter sends out the rays, the shoot and bounce ray tracing method are used to find all the intersections and direction vectors of secondary reflected rays and secondary transmitted rays (STRs), as shown in Figure 4(b).

The secondary rays are traced individually with this recursive ray-tracing method until the specified number of iterations or their reception by the receiver is attained. In the simulation, the receiving antenna is moved across the four layers of the human abdomen model while the transmitter is positioned at the skin's surface. The simulation includes a maximum of ten transmissions and reflections. In the abdomen region, path loss is computed at 1 mm intervals up to a depth of 30 cm.

4. PATH LOSS INSIDE HUMAN ABDOMEN MODEL

We looked at path loss with a KeySight N9917A Vector Network Analyzer (VNA) in a honey-based liquid phantom [16], which is like the human abdomen, to make sure that the proposed antenna design would work as a transmitter for frequencies below and above 6 GHz.

Two proposed antennas were fabricated and used as receiving and transmitting antennas. To prevent any shorts, a polythene cover with a thickness of 0.5 mm is used to insulate the receiving antenna. Figure 5 depicts the measuring configuration. Figure 6 shows the path loss calculated for various depths using the S_{21} parameter. Figure 7 shows the estimated path loss parameters for the human abdomen using the numerical simulation at 5.6, 7.2, and 8.5 GHz, as well as the measurements obtained at the respective frequencies in honey-based liquid phantoms.

Despite using a homogeneous liquid phantom, measured and estimated path loss parameters show good agreement with almost the same slope. Transmitting and receiving antenna misorientation caused variations in the field intensity measurements as the receiving antenna was manually moved through the phantom. To investigate the impact of the DTR path on received field strength, the picture also includes a simulated result without direct transmission (RR + TR).

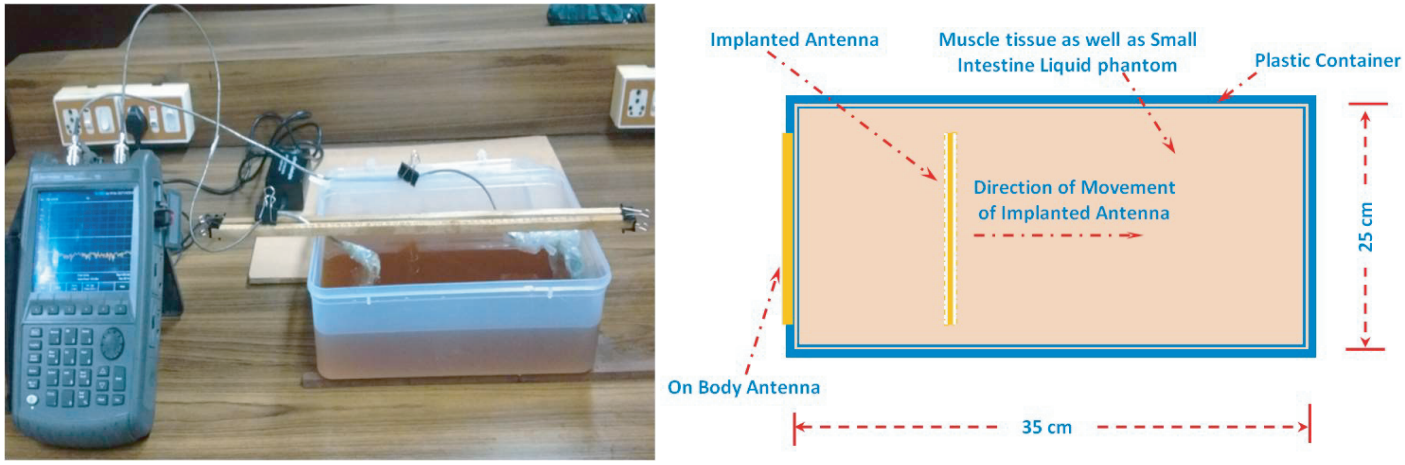

FIGURE 5. Measurement setup for path loss.

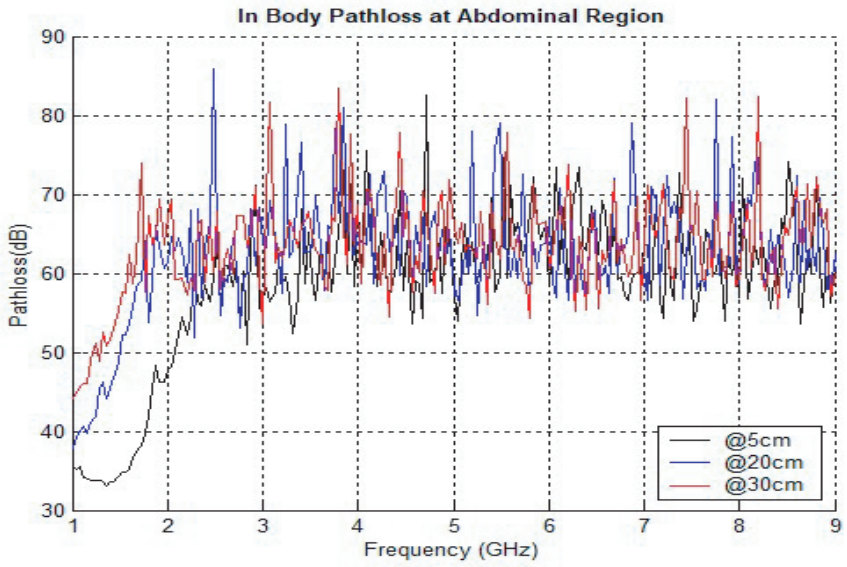

FIGURE 6. Measurement of path loss at various depths.

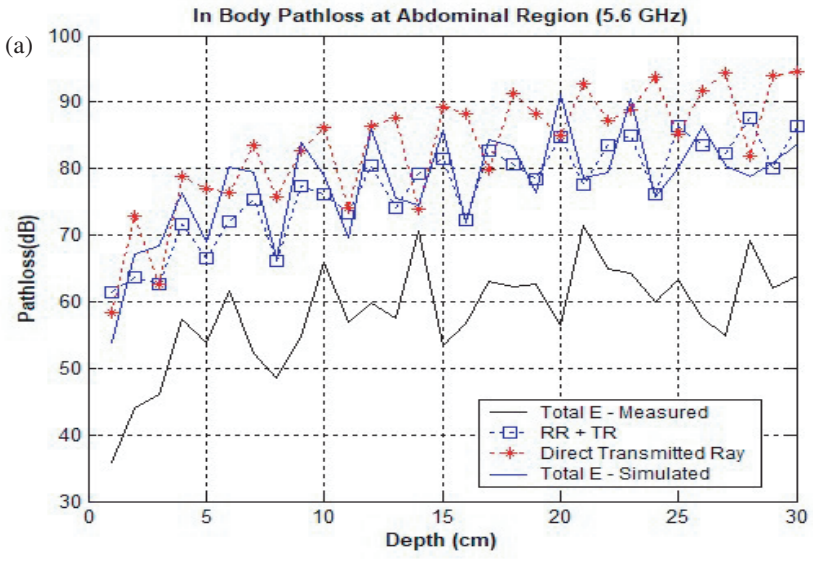

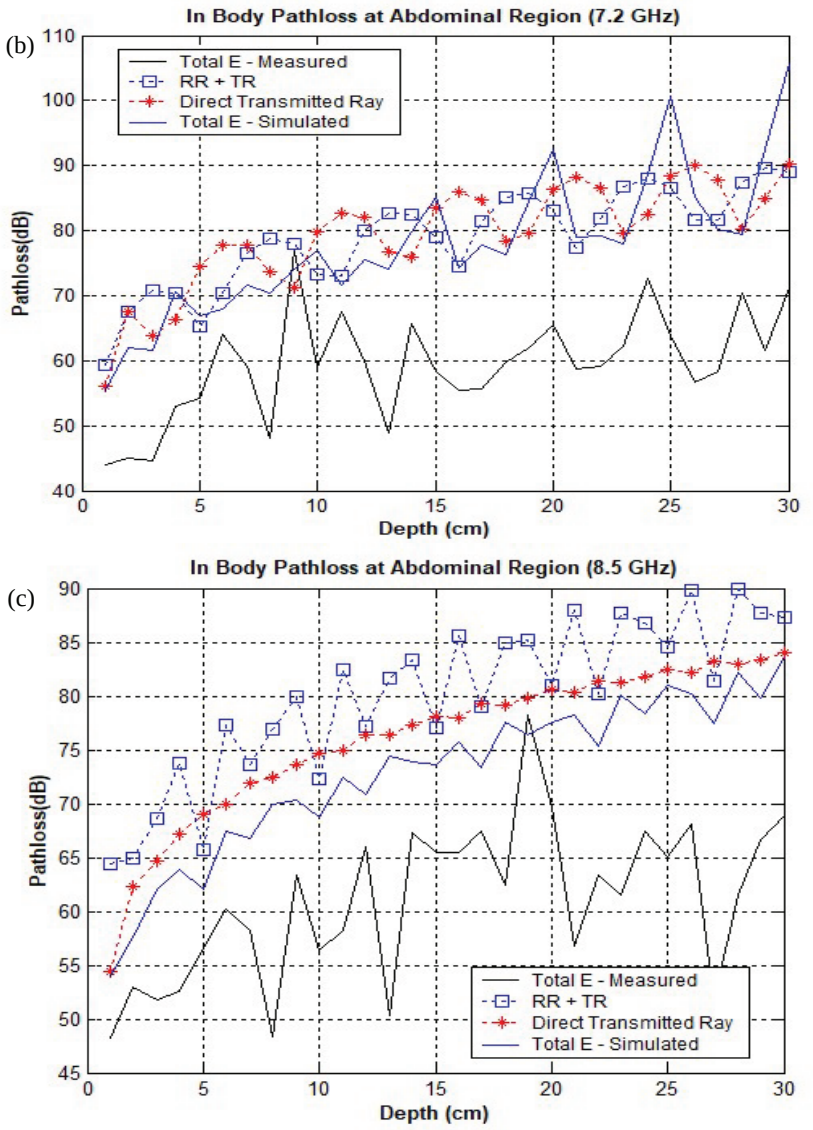

FIGURE 7. Measurement and Simulated path loss at (a) 5.6 GHz, (b) 7.2 GHz and (c) 8.5 GHz.

5. CONCLUSION

For on-body-to-in-body communications, the developed antenna performs effectively for frequencies within and beyond the 6 GHz frequency range. The measurements made in honey-based liquid phantoms at the relevant frequencies are compared to the path loss that would happen in a human belly if the antennas were placed farther apart. The correlation between measured and anticipated path loss parameters is very good. Path loss is lower in the skin and fat layers than in the muscle and small intestinal layers due to their low attenuation constants. The rise in path loss is more obvious at greater antenna separations, according to observations.

REFERENCES

[1] Chavez-Santiago, R. and I. Balasingham, "Ultrawideband signals in medicine [life sciences]," *IEEE Signal Processing Magazine*, Vol. 31, No. 6, 130–136, Nov. 2014.

[2] Zastrow, E., S. K. Davis, and S. C. Hagness, "Safety assessment of breast cancer detection via ultrawideband microwave radar operating in pulsed-radiation mode," *Microwave and Optical Technology Letters*, Vol. 49, No. 1, 221–225, 2007.

[3] Otto, C., A. Milenković, C. Sanders, and E. Jovanov, "System architecture of a wireless body area sensor network for ubiquitous health monitoring," *Journal of Mobile Multimedia*, Vol. 1, No. 4, 307–326, Jan. 2006.

[4] Wang, J. and Q. Wang, "Channel modeling and ber performance of an implant UWB body area link," in *2009 2nd International Symposium on Applied Sciences in Biomedical and Communication Technologies*, 1–4, Bratislava, Slovakia, 2009.

[5] Nagaoka, T., S. Watanabe, K. Sakurai, E. Kunieda, S. Watanabe, M. Taki, and Y. Yamanaka, "Development of realistic high-resolution whole-body voxel models of Japanese adult males and females of average height and weight, and application of models to radio-frequency electromagnetic-field dosimetry," *Physics in Medicine & Biology*, Vol. 49, No. 1, 1–15, 2004.

[6] Khaleghi, A., R. Chávez-Santiago, X. Liang, I. Balasingham, V. C. M. Leung, and T. A. Ramstad, "On ultra wideband chan-

nel modeling for in-body communications," in *IEEE 5th International Symposium on Wireless Pervasive Computing 2010*, 140–145, Modena, Italy, 2010.

[7] Khaleghi, A., R. Chávez-Santiago, and I. Balasingham, "Ultra-wideband statistical propagation channel model for implant sensors in the human chest," *IET Microwaves, Antennas & Propagation*, Vol. 5, No. 15, 1805–1812, Dec. 2011.

[8] Gabriel, C., "Compilation of the dielectric properties of body tissues at RF and microwave frequencies," Ph.D. dissertation, King's College London, United Kingdom, 1996.

[9] Khaleghi, A., R. Chávez-Santiago, and I. Balasingham, "An improved ultra wideband channel model including the frequency-dependent attenuation for in-body communications," in *2012 Annual International Conference of the IEEE Engineering in Medicine and Biology Society*, 1631–1634, San Diego, CA, USA, 2012.

[10] Støa, S., R. Chavez-Santiago, and I. Balasingham, "An ultra wideband communication channel model for the human abdominal region," in *2010 IEEE Globecom Workshops*, 246–250, Miami, FL, USA, 2010.

[11] Støa, S., R. Chavez-Santiago, and I. Balasingham, , "An ultra wideband communication channel model for capsule endoscopy," in *2010 3rd International Symposium on Applied Sciences in Biomedical and Communication Technologies (ISABEL 2010)*, 1–5, Rome, Italy, 2010.

[12] Floor, P. A., R. Chávez-Santiago, S. Brovoll, □. Aardal, J. Bergsland, O.-J. H. N. Grymyr, P. S. Halvorsen, R. Palomar, D. Plettemeier, S.-E. Hamran, T. A. Ramstad, and I. Balasingham, "In-body to on-body ultrawideband propagation model derived from measurements in living animals," *IEEE Journal of Biomedical and Health Informatics*, Vol. 19, No. 3, 938–948, May 2015.

[13] Ishimaru, A., *Electromagnetic Wave Propagation, Radiation, and Scattering: From Fundamentals to Applications*, John Wiley & Sons, 2017.

[14] Seidel, S. Y. and T. S. Rappaport, "Site-specific propagation prediction for wireless in-building personal communication system design," *IEEE Transactions on Vehicular Technology*, Vol. 43, No. 4, 879–891, Nov. 1994.

[15] Rappaport, T. S., *Wireless Communications: Principles and Practice*, Cambridge University Press, 2024.

[16] Thirumaraiselvan, P. and S. Jayashri, "Numerical modelling of ultra wide band signal propagation in human abdominal region," *International Journal of Biomedical Engineering and Technology*, Vol. 27, No. 1-2, 17–32, 2018.

[17] Priya, A., S. K. Mohideen, and P. Thirumaraiselvan, "Propagation losses of UWB antenna for on-body to in-body signal propagation," *Progress In Electromagnetics Research M*, Vol. 73, 101–109, 2018.

[18] Tang, M.-C., R. W. Ziolkowski, and S. Xiao, "Compact hyperband printed slot antenna with stable radiation properties," *IEEE Transactions on Antennas and Propagation*, Vol. 62, No. 6, 2962–2969, Jun. 2014.

[19] Khan, Q. U., D. Fazal, and M. b. Ihsan, "Use of slots to improve performance of patch in terms of gain and sidelobes reduction," *IEEE Antennas and Wireless Propagation Letters*, Vol. 14, 422–425, 2014.

[20] Mok, W. C., S. H. Wong, K. M. Luk, and K. F. Lee, "Single-layer single-patch dual-band and triple-band patch antennas," *IEEE Transactions on Antennas and Propagation*, Vol. 61, No. 8, 4341–4344, Aug. 2013.

[21] Ojaroudi, N., M. Ojaroudi, and N. Ghadimi, "Dual band-notched small monopole antenna with novel W-shaped conductor backed-plane and novel T-shaped slot for UWB applications," *IET Microwaves, Antennas & Propagation*, Vol. 7, No. 1, 8–14, 2013.

[22] Li, P., J. Liang, and X. Chen, "Study of printed elliptical/circular slot antennas for ultrawideband applications," *IEEE Transactions on Antennas and Propagation*, Vol. 54, No. 6, 1670–1675, Jun. 2006.

[23] Chen, W.-L., G.-M. Wang, and C.-X. Zhang, "Bandwidth enhancement of a microstrip-line-fed printed wide-slot antenna with a fractal-shaped slot," *IEEE Transactions on Antennas and Propagation*, Vol. 57, No. 7, 2176–2179, Jul. 2009.

[24] Gupta, A. and V. Kumar, "Design of a tri-band patch antenna with back reflector for off-body communication," *Wireless Personal Communications*, Vol. 115, No. 1, 173–185, 2020.

[25] Mol, J. M. S., S. E. Florence, and M. Abraham, "Twisted F-shaped slot loaded UWB printed antenna for on-body application," *Wireless Personal Communications*, Vol. 124, No. 3, 2427–2445, 2022.

[26] Seydi, M. and M. S. Bayati, "Design, simulation and fabrication of an implanted antenna at ISM band in body tissue," *Wireless Personal Communications*, Vol. 122, No. 3, 2023–2033, 2022.